



# Maintenance condition of back-building squall-line in a numerical simulation of a heavy rainfall event in July 2010 in Western Japan

Yoshida, Ryuji ; Nishizawa, Seiya ; Yashiro, Hisashi ; Adachi, Sachiho A. ; Yamaura, Tsuyoshi ; Tomita, Hirofumi ; Kajikawa, Yoshiyuki

---

(Citation)

Atmospheric Science Letters,20(1):e880-e880

(Issue Date)

2019-01

(Resource Type)

journal article

(Version)

Version of Record

(Rights)

© 2018 The Authors. Atmospheric Science Letters published by John Wiley & Sons Ltd on behalf of the Royal Meteorological Society.

This is an open access article under the terms of the Creative Commons Attribution License, which permits use, distribution and reproduction in any medium, provided th...





(URL)

<https://hdl.handle.net/20.500.14094/90005529>



## RESEARCH ARTICLE

# Maintenance condition of back-building squall-line in a numerical simulation of a heavy rainfall event in July 2010 in Western Japan

Ryuji Yoshida<sup>1,2,3,4</sup>  | Seiya Nishizawa<sup>4</sup>  | Hisashi Yashiro<sup>4</sup> | Sachiho A. Adachi<sup>4</sup>  |  
Tsuyoshi Yamaura<sup>3,4</sup> | Hirofumi Tomita<sup>4,5</sup> | Yoshiyuki Kajikawa<sup>3,4</sup> 

<sup>1</sup>CIRES, University of Colorado Boulder, Boulder, Colorado

<sup>2</sup>NOAA Earth System Research Laboratory, Boulder, Colorado

<sup>3</sup>Research Center for Urban Safety and Security, Kobe University, Kobe, Japan

<sup>4</sup>Computational Climate Science Research Team, RIKEN Center for Computational Science, Kobe, Japan

<sup>5</sup>Japan Agency for Marine-Earth Science and Technology, Yokohama, Japan

## Correspondence

Ryuji Yoshida, CIRES/University of Colorado, NOAA/ESRL, 325 Broadway, Boulder, CO 80305.

Email: ryuji.yoshida@noaa.gov

## Funding information

HPCI Junior Researcher Promotion Project, Grant/Award Number: hp170164; Japan Science and Technology Agency (JST) Core Research for Evolutional Science and Technology (CREST), Grant/Award Number: JPMJCR1312; Foundation for Computational Science (FOCUS) Establishing Supercomputing Center of Excellence

Back-building squall-lines (BBSs) cause local heavy rainfalls and lead to natural disasters. Therefore, better understanding BBSs would have a significant impact on disaster prevention and mitigation. Although a conceptual maintenance condition of BBSs is proposed by previous studies, the concept stands on a case study. We clarified that a mesoscale moist area in water vapor front localizes the continuous forming of new cells in the BBS and reinforced the concept with another case. A numerical simulation of the heavy rainfall during July 11–12, 2010, in western Japan was used to confirmation of the conceptual maintenance condition of the BBS. We found that the new cells of BBS are continually formed at the confluence zone of the synoptic-scale cold front and the mesoscale area with large water vapor amount at low-level. It supports the conceptual maintenance condition, and the mesoscale moist area in water vapor front is a distinct characteristic in this case. The position where new cells are formed has been anchored by the mesoscale moist area for 2 hr.

## KEYWORDS

back-building squall-line, mesoscale, mesoscale convective systems, regional mesoscale modeling, severe weather

## 1 | INTRODUCTION

Quasi-stationary mesoscale convective systems (MCSs) so-called as back-building squall-lines (BBSs) cause heavy rainfalls over Japan and lead to natural disasters. In BBSs, the convective cells are arranged in a line along the mid-upper wind direction. Newer cells appear on the upwind side, which is the opposite side of the cell motion (Bluestein and Jain, 1985; Parker and Johnson, 2000). Environment of rich low-level moisture is necessary for heavy rainfall including BBSs, and mid-level moisture is also suitable condition (Chuda and Niino, 2005; Tsuguti and Kato, 2014;

Unuma and Takemi, 2016). These environments tend to develop in the early summer season from June to July called as Baiu season. In Baiu season, BBSs are observed around a stationary front, namely Baiu front (Yoshizaki *et al.*, 2000; Kato, 2006; Shinoda *et al.*, 2009), because the southern part of Baiu front has a rich low-level moisture. The north–south gradient of water vapor (WV) amount is introduced as WV front in Moteki *et al.* (2004a).

The large-scale environments of BBSs have been investigated, however, the maintenance condition of BBSs is still not clearly understood. Formation of new cells at upwind side is essential to maintain back-building structure, and a

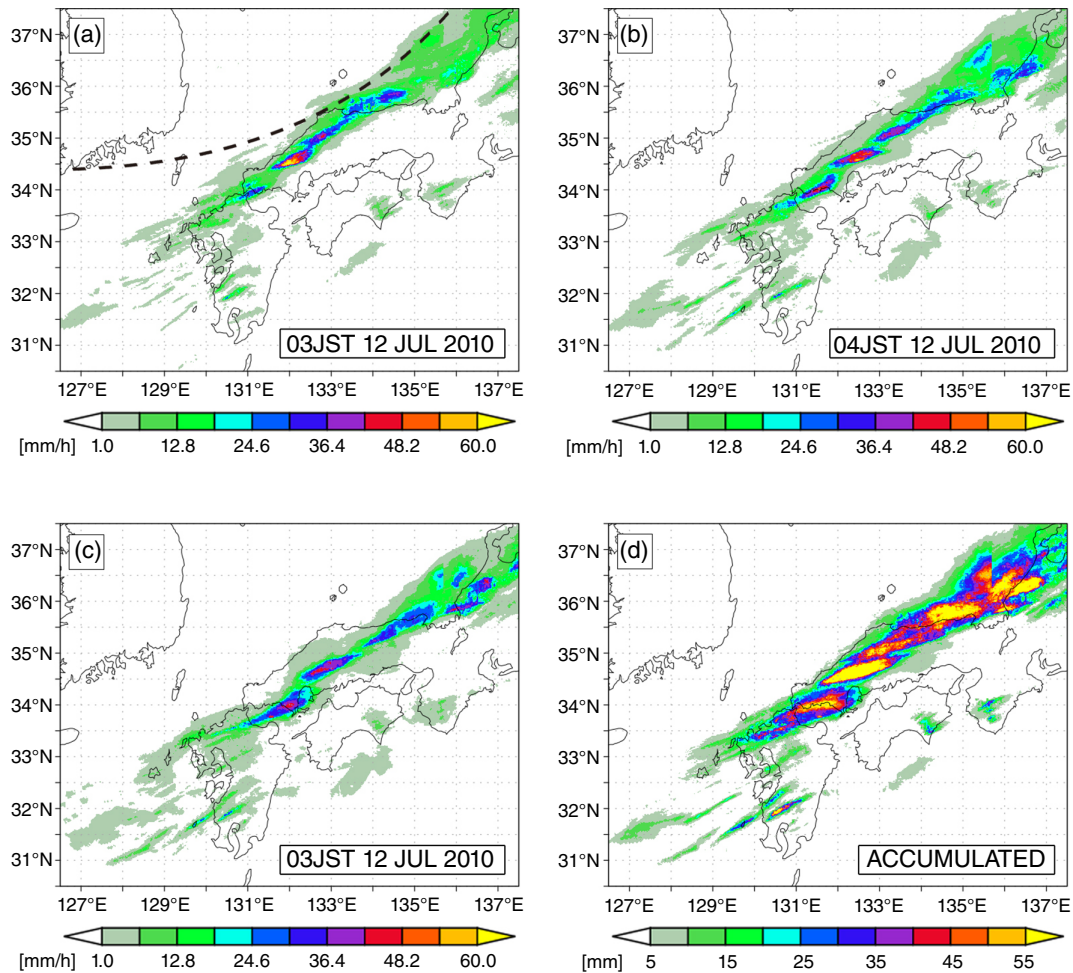


**FIGURE 1** Radar/Rain gauge-Analyzed Precipitation data provided by the JMA for the period from 03:00 JST to 05:00 JST on July 12, 2010 for (a-c). (d) is an accumulated precipitation in the same period from 03:00 JST to 06:00 JST. A linear precipitation area with a south-west to north-east orientation is observed. The broken line in (a) shows the surface location of the synoptic-scale cold front, on a weather map provided by the JMA, at 03:00 JST on July 12, 2010

condition to maintain continuous updrafts is necessary to form new cells. In this study, the location where new cells are formed is referred to as an initiation point. The initiation point would have some mesoscale characteristics to localize continuous updrafts. In some of the BBSs formed over Japan, continuous updrafts are formed due to the effect of topographic barriers (Yoshizaki *et al.*, 2000). When the effect of topography on BBS is not dominant, a convergence affected by the temperature contrast over the synoptic-scale front is a possible reason for the formation of an updraft (Kato and Goda, 2001). Synoptic-scale front may cause wind shear. Magnitude of wind shear over deep layer of troposphere is significantly stronger for mature MCSs than for weakening MCSs (Coniglio *et al.*, 2007). However, the synoptic-scale front is too large to specify the initiation

point. For enhancement of initiated convections, the synoptic-scale front is not often sufficient and low-level warm air advection is fundamental feature in growing MCSs (Jirak and Cotton, 2007). Peters and Schumacher (2016) distinguished an internal (smaller-scale) environmental effect from an external (larger-scale) environmental effect. They found that the internal environments affect to become a long-lasting MCS. Moteki *et al.* (2004a) proposed a conceptual maintenance condition of BBS in Japan, which is a confluence zone of Baiu front and WV front. Similar conditions

**TABLE 1** Computational domain settings

Items	Domain 1	Domain 2	Domain 3
Domain arrangement	Outermost	Intermediate	Innermost
Horizontal grid-spacing (km)	7.5	2.5	0.5
Vertical levels	48	60	80
Model top height (km)	30	28	24

**TABLE 2** Summary of physics scheme used in the simulation

Items	Settings
Microphysics	Six-category one-moment bulk scheme (Tomita, 2008)
Radiation	A correlated k-distribution scheme (Sekiguchi and Nakajima, 2008)
PBL turbulence	MYNN level 2.5 scheme (Nakanishi and Niino, 2009)
Land and sea surface	A similarity scheme (Beljaars and Holtslag, 1991; Wilson, 2001)
Land process	A diffusion and bucket model
Sea process	Slab Ocean model
Urban process	A single layer urban canopy model (Kusaka <i>et al.</i> , 2001)

are found in BBSs over the northern Kyusyu area over Japan (Kato, 2006). A mesoscale cold pool locally strengthens a temperature gradient on Baiu front, and the temperature gradient localizes the continuous updraft on the confluence zone (Moteki *et al.*, 2004b). However, this conceptual

maintenance condition is suggested based on a case study. A cause for localization of continuous updraft has not been fully understood yet. Therefore, a confirmation of conditions in another BBS case is necessary to consolidate the conceptual maintenance condition.

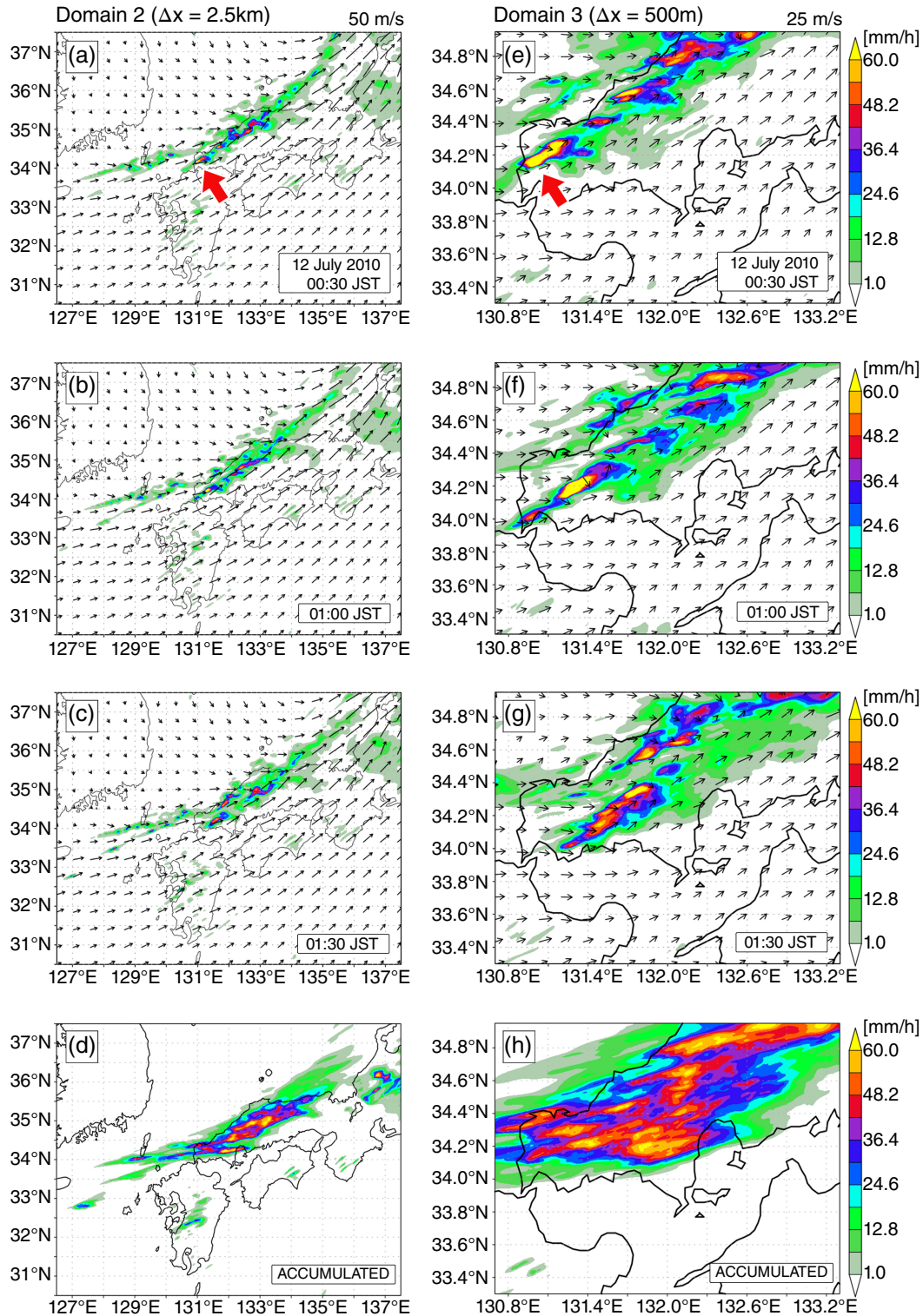


**FIGURE 2** Horizontal distribution of simulated precipitation from 00:30 JST to 01:30 JST, July 12, 2010 for (a–c) and (e–g). (d) and (h) are accumulated precipitation in the period from 00:00 JST to 03:00 JST. (a–d) are results in Domain 2; and (e–g) are results in Domain 3. Vectors represent horizontal wind at 2 km height, but the vectors in (e–g) are horizontal wind anomalies relative to the area average of Domain 2 representing a synoptic-scale environment. A linear precipitation area that is similar to the observations is simulated. In (a) and (e), the red arrow indicates the location of the initiation point of new cells



We selected a heavy rainfall event in western Japan in July 2010. The typical back-building structure was found in this event, while the precipitation magnitude of this event is weaker than that in Moteki *et al.* (2004a). Figure 1 shows the horizontal distribution of precipitation using Radar/Rain-gauge-Analyzed Precipitation data provided by Japan Meteorological Agency (JMA). A quasi-stationary rainband with a south-west to north-east orientation was observed, and the

rainband consisted of several BBSs. The rainband caused an extreme precipitation rate of over 60 mm/hr and an accumulated precipitation of more than 50 mm in 3 hr from 03:00 Japan Standard Time (JST) to 06:00 JST on July 12, 2010. A Baiu front merged with a synoptic scale cold front was analyzed on the weather map; it was located on the north of the rainband over the Japan Sea. Southwesterly wind was observed over the south of the Baiu front. These are

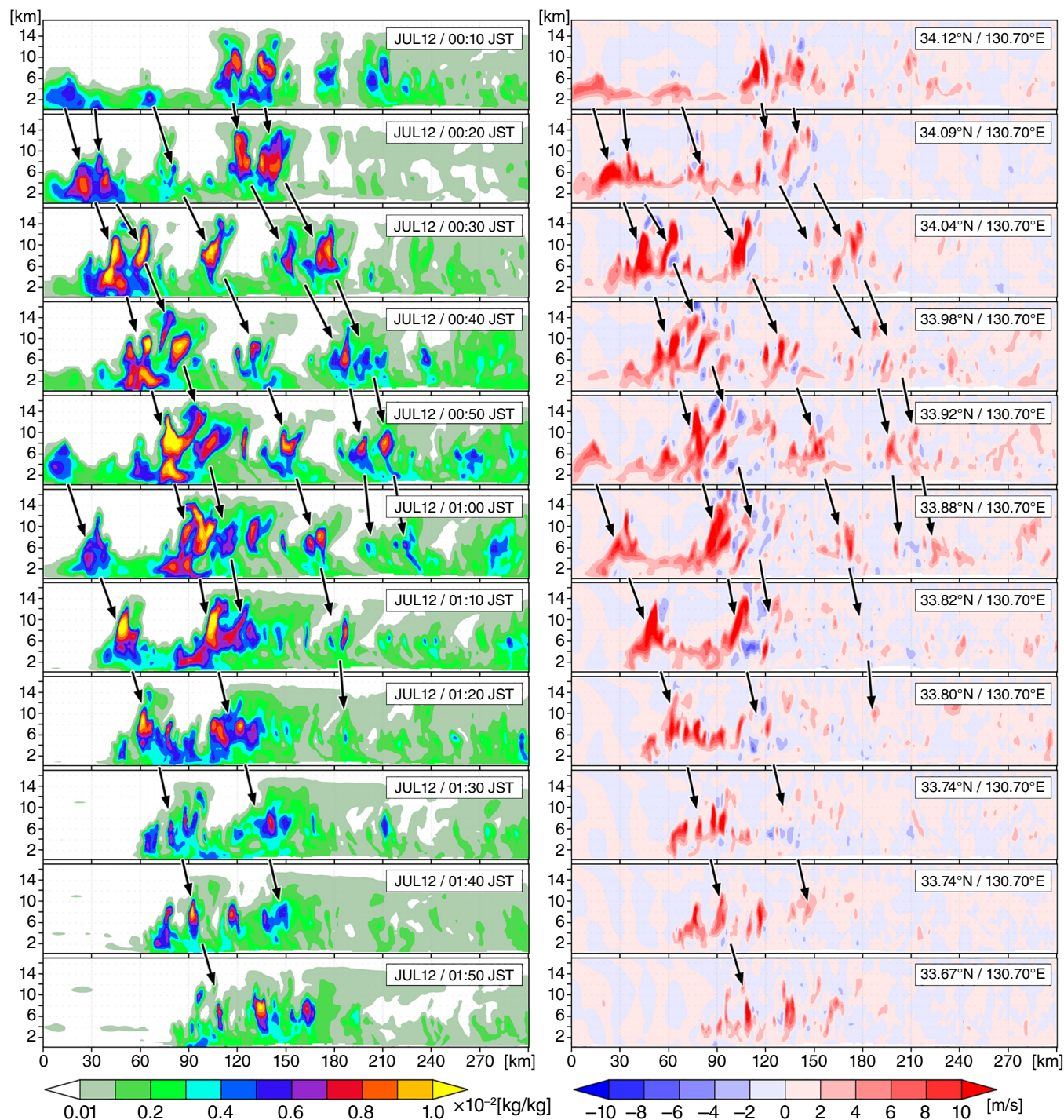


**FIGURE 3** Vertical-longitudinal cross section for hydrometeors amounts on the left and vertical wind speed on the right following the squall-line. Hydrometeors are defined as the sum of the mixing ratios of cloud water, rain droplets, cloud ice, snow, and graupel at each level. Each cross section is along the linear shape of squall-line, and the squall-line is determined subjectively by observing the precipitation for the period from 00:10 JST to 01:50 JST on July 12, 2010. Latitude and Longitude information are locations on the map in the left edge of each panel. Black arrows trace the movement of each cell

consistent with synoptic-scale environments reported in Moteki *et al.* (2004a). It was determined from 1 hr interval snapshots of radar images that intense convections were located on the south-western side of the BBS.

## 2 | NUMERICAL SIMULATION SETTINGS

We performed a numerical simulation of the BBS by using one-way triple nested computational domains (Figure S1, Supporting Information). The Scalable Computing for Advanced Library Environment-Regional Model (SCALE-RM; Nishizawa *et al.*, 2015; Sato *et al.*, 2015) was used for the numerical simulation. SCALE-RM is well optimized to use on massive parallel supercomputers, and can provide possibilities for higher resolution simulation. Tables 1 and 2 show summaries of the computational domain settings and the physics schemes, respectively.

The grid point value of the global spectral model provided by the JMA (GSM-GPV) for Japan area ( $1^\circ$  grid

spacing with 30 levels, 3hr) were used as an initial condition for all the domains and as a boundary condition for Domain 1. The boundary conditions for Domain 2 and Domain 3 were created by using the cost-effective online nesting procedure (CONeP; Yoshida *et al.*, 2017). The integration period was from 09:00 JST on July 10, 2010 to 09:00 JST on July 12, 2010. A spin-up period of 24 hr was taken before the occurrence of the heavy rainfall in order to organize the BBS in the model.

## 3 | OUTLINE OF THE SIMULATED BACK-BUILDING SQUALL-LINE

Figure 2 shows the horizontal distribution of precipitation in Domain 2 and Domain 3 from 00:30 JST to 01:30 JST on July 12, 2010. Although the simulated rainband is formed a little earlier and weaker than the observation, a distribution of accumulated precipitation for 3 hr from 00:00 JST to 03:00 JST is similar to that observed in Figure 1d. The linear

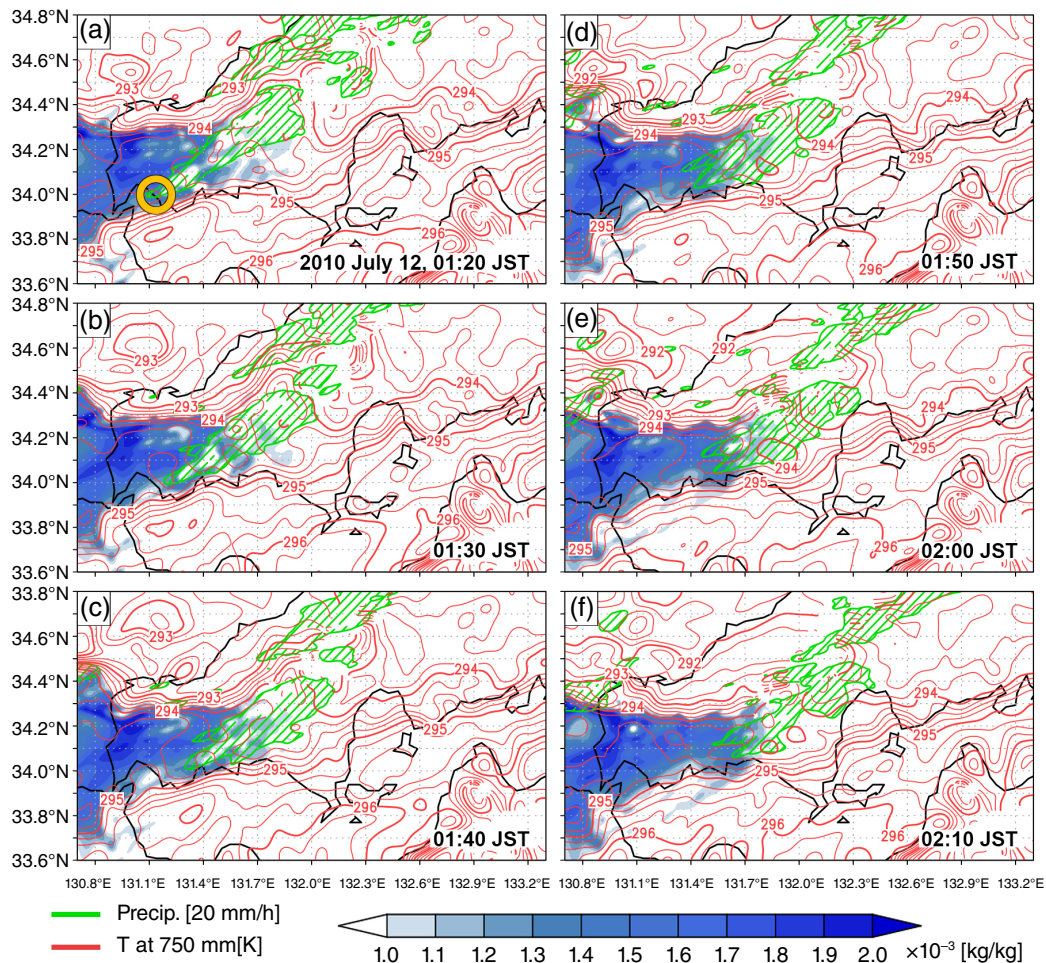


**FIGURE 4** Positional relationship between cold fronts and moist air. Areas within green contours have a precipitation rate of 20 mm/hr (inner area is hatched) and the red contours represent the temperature at 750 m height. A horizontal spatial filter of 100 km scale is applied to the temperature measurements in order to clearly show the synoptic-scale cold front. The color scale shows the residual specific humidity ( $Q_v$ ) relative to the average specific humidity of the area (0.016 kg/kg). Only positive residual specific humidity is visualized; shaded areas have higher moisture content than the average specific humidity of the area



shaped structure and the quasi-stationary characteristic of the rainband are simulated. In the simulation, an extreme precipitation rate of over 60 mm/hr was observed in Domain 3. A thermodynamic profile and a wind profile are well simulated comparing with the radio-sonde observation and the JMA GSM-GPV data at the Fukuoka observation station (Figure S2). As shown in Figure 2a–c, the weak northern wind over the Japan Sea and the southwesterly wind in the south area of the simulated rainband are found. At mid- and upper-levels, the westerly wind prevails. The simulated rainband consists of multiple BBSs similarly to the observed rainband. In this study, we focused on the BBS located at upwind side in the rainband to avoid contaminations among BBSs (indicated by a red arrow in Figure 2).

To investigate the detailed structure of the BBS, we drew vertical cross section images for hydrometeors ( $Q_{\text{hyd}}$ ) and vertical wind speed as shown in Figure 3. The  $Q_{\text{hyd}}$  is the sum of the mixing ratios of cloud water, rain droplets, cloud ice, snow, and graupel. Cross sections are drawn along a major axis of the linear shape of the BBS by subjectively following the BBS based on precipitation distributions. It is clear that the BBS is composed of multiple cells. The lifetime of each cell is approximately 60 to 80 min.  $Q_{\text{hyd}}$  on the western side of the BBS are concentrated at the mid-level while those on the eastern side are concentrated at the upper-level. An updraft from the low-level to upper-level is observed on the western side. However, less significant updraft is observed on the eastern side. Thus, new cells are formed at the western end of the BBS and move eastwards during its life; the cells located on the eastern side are older than those on the western side. Therefore, we defined the western end of the BBS as the initiation point. These cell characteristics are consistent with those of the typical BBS in Bluestein and Jain (1985).

#### 4 | A CONDITION FOR MAINTAINING UPDRAFT AT THE INITIATION POINT

The numerical model simulated a BBS, and updraft at the initiation point was maintained. Some specific features triggering and maintaining updrafts should be found around the initiation point. First, we investigated the low-level thermodynamic environment. Figure 4 shows the horizontal distribution of WV and temperature at 750 m height in Domain 3. The initiation point is indicated by the yellow circle in Figure 4a. The synoptic-scale cold front is found as two cold fronts at 01:20 JST on July 12, 2010, as indicated by the concentration of temperature contours in Figure 4a. The cold fronts are found at temperatures around 293 and 295 K. Over the south-westerly wind area in Figure 2e–g, WV amount (specific humidity) is larger than 0.014 kg/kg. Furthermore, the meso-scale moist area (MMA) is found in the WV front. The area with WV amounts higher than the mean WV amounts of the Domain 3 (0.016 kg/kg) is shaded in

Figure 4, and it corresponds to the MMA. The WV is advected from the south-west by the low-level jet reported in Nagata and Ogura (1991) and concentrated at the MMA. That is, the initiation point is located over the mesoscale confluence zone of the synoptic-scale cold fronts and the MMA. The confluence zone is maintained from 00:10 JST to 02:10 JST and the initiation point is located over the confluence zone. In the confluence zone, a forced ascent would be induced by the convergence of the synoptic-scale cold fronts. The ascent flow would be accelerated by the diabatic heating in the convection with rich WV. The confluence zone might provide essential conditions for triggering and acceleration of the updraft, and thus the updraft can be maintained at the confluence zone. Since the synoptic-scale cold front moves south-eastward slowly and the MMA is quasi-stationary, the confluence zone is almost stationary. Therefore, the updraft occurs at the same point. The confluence zone found in this simulation is similar to the conceptual

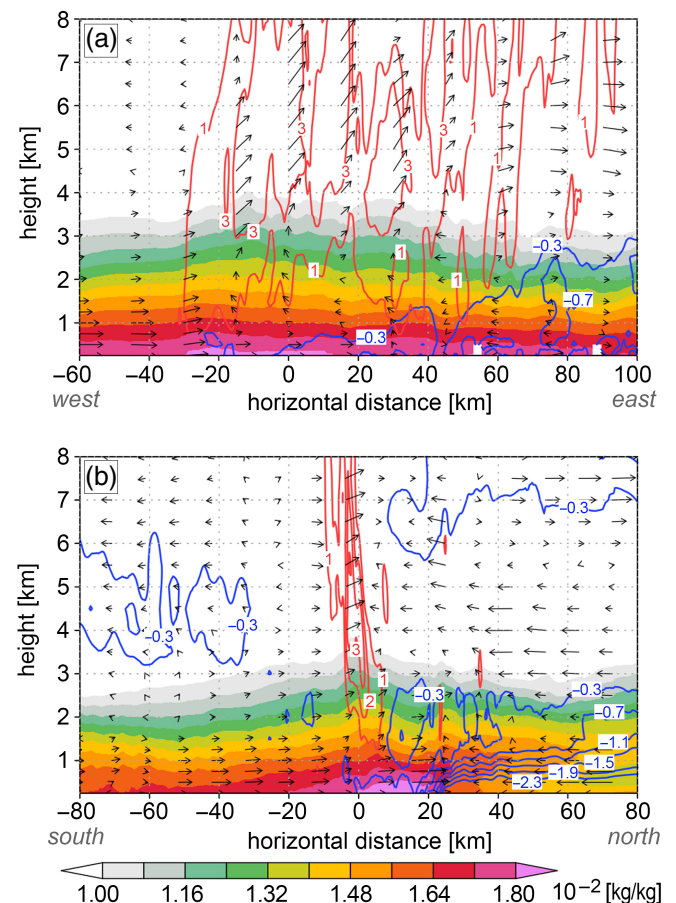


**FIGURE 5** Temporal composited images for specific humidity (color scale), vertical velocity [m/s] (red contours), and temperature [K] (blue contours). (a) is the parallel component and (b) is the orthogonal component relative to the direction of the linear shape of the squall-line. Vectors show flow fields on each plane. Temperature data are shown as anomalies relative to the domain average. The composite center indicated as 0 km is defined as the point at which the maximum vertical velocity is observed at the time in the simulated squall-line represented by precipitation. Each center is determined subjectively by observing the squall-line for the period from 00:10 JST to 02:00 JST on July 12, 2010 (12 snapshots)

maintenance condition in Moteki *et al.* (2004a). In detail, however, a mesoscale cold pool in the synoptic-scale front is not found in this case, and the MMA is found in the WV front. An interface between a synoptic-scale cold front and a low-level warm air advection is emphasized as a significant environment for MCSs development over the North America by Augustine and Caracena (1994). This environmental condition is similar to the confluence zone found in this study.

Next, we drew the vertical cross sections shown in Figure 5 to confirm relationship between the updraft and the mesoscale confluence zone. These are divided into a parallel- and an orthogonal-component relative to the major axis of the BBS linear shape. The direction of the major axis was determined by the precipitation contour lines. Figure 5 is a temporal composite of 12 snapshots taken during the period from 00:10 JST to 02:00 JST on July 12, 2010, centered on the location at which the maximum vertical velocity was observed in the air column on the BBS. The location of this center is determined subjectively. In the parallel component (Figure 5a), the updraft is observed above the synoptic-scale cold front. Although the maximum vertical velocity is located at a horizontal distance of 0 km, the low-level updraft can be found 20 km to the west. While a broad updraft is observed in the parallel component, the updraft is found at a particular area around the 0 km point in the orthogonal component. This implies the BBS has narrow structure in the north–south direction. Interestingly, WV is also concentrated at the point of  $-20$  km, where the MMA is found. The maximum WV amount is  $0.018$  kg/kg for the specific area between 0 and 20 km. Inflow from the south (west) to the BBS is dominant than from the north (east). The inflow passes through the MMA before reaches the BBS. Furthermore, at slightly higher level than the inflow, the synoptic-scale cold front is significant at a horizontal distance of 20 km with a large temperature gradient of approximately  $2$  K per  $0.1^\circ$ . These amounts are similar to that observed over the Baiu front in Moteki *et al.* (2004a). The confluence zone is also clearly found in the vertical cross-sections in the area between 0 km and 20 km in Figure 5b. These structures imply that the updraft is initiated at the confluence zone. This is maintained for the period from 00:10 JST to 02:00 JST on July 12, 2010. Since the standard deviations of the composited samples are approximately 10% of the averaged value, the composited fields represent the mean structure of the simulated BBS. The images imply that the process continuously occurs for this period and reinforces the maintenance condition discussed above.

In this case, the MMA is newly found as the mesoscale characteristic of the maintenance condition. We confirmed the necessity of the MMA to maintain the BBS by a restart experiment with a less WV condition (LWV) than the real case. We call the original simulation as a control experiment (CTL). The restart time was 00:00 JST on July 12, 2010, when the BBS was just organized. The mass of

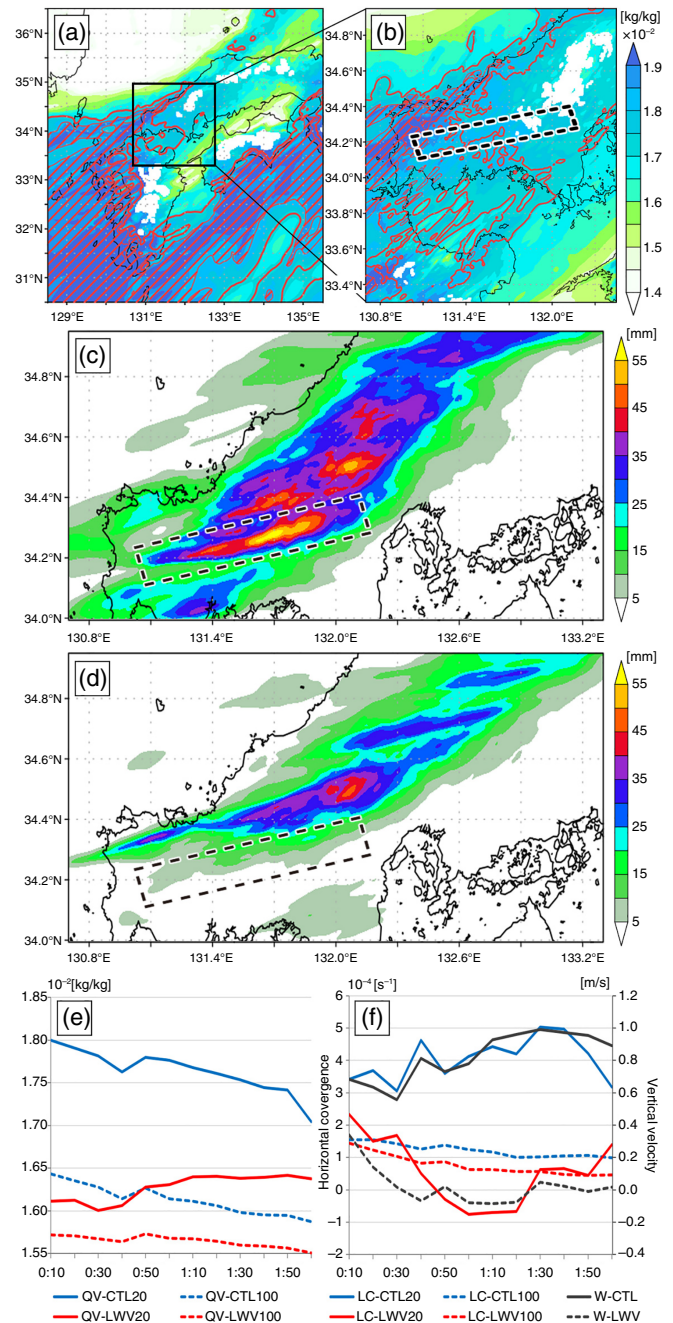


**FIGURE 6** Result of a less water vapor experiment (LWV). (a) and (b) are conditions of a restart simulation for Domain 2 and Domain 3, respectively. A location of the BBS which is focused on is indicated by a rectangle in (b). Color shade shows  $QV_{CTL}$  at 750 m height. Contour is difference of specific humidity (QV) at 750 m height at value of  $0.001$  kg/kg, and hatched areas are larger difference than  $0.002$  kg/kg. (c) and (d) are accumulated precipitation in the period from 00:20 JST to 01:40 JST on July 12, 2010; (c) is control run (CTL), and (d) is LWV. A location of the BBS which is focused on is indicated by a rectangle in (c), and the same location is indicated in (d). (e) and (f) are area averaged time series for QV at 500 m height, low-level convergence (LC) at 500 m height, and W (vertical velocity) at 3,000 m height. For lines colored by blue or red, solid-lines and dashed-lines are area averaged values in the area of 20 km radius and 100 km radius, respectively. W is area averaged in the area of 20 km radius, and black solid-line and black dashed-line are for CTL and LWV, respectively. The center of area averaging is decided by the BBS tracking in a same manner of Figure 5



WV is defined as  $\rho Q_v$  kg/m<sup>3</sup> ( $\rho$  is density, and  $Q_v$  is WV in specific humidity) and was decreased to the area mean value, which is averaged in each computational domain at the all levels in 0–4 km height. The difference of  $Q_v$  from LWV to CTL at 750 m height is shown in Figure 6a,b.  $Q_v$  is decreased in the limited area with high  $Q_v$  in Domain 3 (Figure 6b). The east–west contrast of WV disappeared by the decreasing process, but the north–south contrast of WV was not eliminated. It is clear that a precipitation from the BBS is not simulated in LWV shown in Figure 6d comparing with Figure 6c. Vertical velocity is also weak in LWV (Figure 6f). It is confirmed by 10 min interval snapshots that the BBS is rapidly decayed by 00:30 JST on July 12 in LWV. The difference of  $Q_v$  and in low-level convergence between LWV and CTL is significantly larger in 20 km area averaging values (solid-lines) than that in 100 km area averaging values (dashed-lines). Therefore, the smaller-scale condition was altered by reducing WV amount, but the larger-scale condition was not much modified. Peters and Schumacher (2016) also claimed that the smaller-scale condition has larger effect to maintain the MCS than larger-scale condition. To recognize the role of  $Q_v$ , we diagnosed acceleration terms of vertical velocity ( $w$ ) at the same location as Figure 6 by following Fovell and Tan (1998). The governing equation is  $\frac{\partial w}{\partial t} = -\mathbf{V} \cdot \nabla w - \frac{1}{\bar{\rho}} \frac{\partial p'}{\partial z} + B'$ , same as Equation 1 in Fovell and Tan (1998). The first term and the second term in the right-hand side are vertical velocity advection (WADV) and vertical pressure gradient (VPGA), respectively.  $\bar{\rho}$  is the base-state density defined as a domain average value.  $B'$  is perturbation buoyancy (BUOY) defined as  $g((\bar{\rho} - \rho')/\rho')$ , where  $g$  is gravitational acceleration.  $p'$  and  $\rho'$  are perturbation pressure and perturbation density defined as 20 km area averaged values. To see the general feature, the values are temporary and vertically averaged in the same time period as Figure 6 and in updraft levels (from 3.25 to 7.75 km height). BUOY terms are  $1.9 \times 10^{-2}$  ms<sup>-2</sup> in CTL and  $8.2 \times 10^{-3}$  ms<sup>-2</sup> in LWV, whereas VPGA terms are  $2.1 \times 10^{-2}$  ms<sup>-2</sup> in CTL and  $4.1 \times 10^{-2}$  ms<sup>-2</sup> in LWV. BUOY term in LWV is one order smaller than that in CTL. WADV terms are three orders less than other terms. Therefore, the less  $Q_v$  condition in LWV leads to less vertical acceleration by buoyancy than CTL and the updraft would not be enough accelerated in LWV to maintain the BBS. This implies that the MMA, that is, local contrast of WV is necessary to maintain the BBS in this case.

## 5 | SUMMARY

Moteki *et al.* (2004a) suggested a conceptual maintenance condition for the BBSs, which is a confluence zone between the Baiu front (temperature gradient) and the water vapor front. However, the conceptual maintenance condition is

ground on the case study, and the updraft localization has not been fully understood. We confirmed the conceptual maintenance condition in another BBS case during June 11–12, 2010, in western Japan by carrying out a numerical simulation. The updraft at the initiation point of the simulated BBS is maintained over the confluence zone of the synoptic-scale cold fronts and the mesoscale distinctive moist area at low-level. In a sensitivity experiment with locally decreased water vapor, the simulated BBS was not maintained. This suggests that a mesoscale distinctive moist area is essential to maintain the simulated BBS in this case. This simulated BBS and its condition support the conceptual maintenance condition of Moteki *et al.* (2004a). A cold pool, that is, a local minimum of temperature in a cold front emphasized in Moteki *et al.* (2004b) is not observed in this case.

## ACKNOWLEDGEMENTS

We are grateful to the editor of ASL and anonymous reviewers for their useful and critical comments. We are grateful to Prof. Satoru Oishi in RCUSS Kobe University for valuable insights. We appreciate Mr Kazuto Ando for technical supports. The Radar/Raingauge-Analyzed Precipitation data and the GSM-GPV data were provided by JMA through the Japan Meteorological Business Support Center. This research used computational resources of the K computer provided by RIKEN through HPCI Junior Researcher Promotion Project (ID: hp170164). This work was supported by JST CREST grant number JPMJCR1312, Japan and FOCUS Establishing Supercomputing Center of Excellence.

## ORCID

Ryuji Yoshida  <https://orcid.org/0000-0003-3238-2595>

Seiya Nishizawa  <https://orcid.org/0000-0001-9457-7457>

Sachiho A. Adachi  <https://orcid.org/0000-0002-3066-6175>

Yoshiyuki Kajikawa  <https://orcid.org/0000-0001-6863-1720>

## REFERENCES

- Augustine, J.A. and Caracena, F. (1994) Lower-tropospheric precursors to nocturnal MCS development over the central United States. *Weather and Forecasting*, 9, 116–135.
- Beljaars, A.C.M. and Holtlag, A.A.M. (1991) Flux parameterization over land surfaces for atmospheric models. *Journal of Applied Meteorology*, 30, 327–341.
- Bluestein, B.H. and Jain, M.H. (1985) Formation of mesoscale line of precipitation: severe squall lines in Oklahoma during the spring. *Journal of the Atmospheric Sciences*, 42, 1711–1732.
- Chuda, T. and Niino, H. (2005) Climatology of environmental parameters for mesoscale convections in Japan. *Journal of the Meteorological Society of Japan*, 83, 391–408.
- Coniglio, M.C., Brooks, H.E., Weiss, S.J. and Corfidi, S.F. (2007) Forecasting the maintenance of quasi-linear mesoscale convective systems. *Weather and Forecasting*, 22, 556–570.
- Fovell, R.G. and Tan, P. (1998) The temporal behavior of numerically simulated multicell-type storms. Part II: the convective cell life cycle and cell regeneration. *Monthly Weather Review*, 126, 551–577.

- Jirak, I.L. and Cotton, W.R. (2007) Observational analysis of the predictability of mesoscale convective systems. *Weather and Forecasting*, 22, 813–838.
- Kato, T. (2006) Structure of the band-shaped precipitation system inducing the heavy rainfall observed over Northern Kyushu, Japan on 29 June 1999. *Journal of the Meteorological Society of Japan*, 84, 129–153.
- Kato, T. and Goda, H. (2001) Formation and maintenance processes of a stationary band-shaped heavy rainfall observed in Niigata on 4 August 1998. *Journal of the Meteorological Society of Japan*, 79, 899–924.
- Kusaka, H., Kondo, H., Kikegawa, Y. and Kimura, F. (2001) A simple single-layer urban canopy model for atmospheric models: comparison with multi-layer and slab models. *Boundary-Layer Meteorology*, 101, 329–358.
- Moteki, Q., Uyeda, H., Maesaka, T., Shinoda, T., Yoshizaki, M. and Kato, T. (2004a) Structure and development of two merged Rainbands observed over the East China Sea during X-BAIU-99 part I: Meso- $\beta$ -scale structure and development processes. *Journal of the Meteorological Society of Japan*, 82, 19–44.
- Moteki, Q., Uyeda, H., Maesaka, T., Shinoda, T., Yoshizaki, M. and Kato, T. (2004b) Structure and development of two merged Rainbands observed over the East China Sea during X-BAIU-99 part II: Meso- $\alpha$ -scale structure and build-up processes of convergence in the Baiu frontal region. *Journal of the Meteorological Society of Japan*, 82, 45–65.
- Nagata, M. and Ogura, Y. (1991) A modeling case study of interaction between heavy precipitation and a low-level jet over Japan in the Baiu season. *Monthly Weather Review*, 119, 1309–1336.
- Nakanishi, M. and Niino, H. (2009) Development of an improved turbulence closure model for the atmospheric boundary layer. *Journal of the Meteorological Society of Japan*, 87, 895–912.
- Nishizawa, S., Yashiro, H., Sato, Y., Miyamoto, Y. and Tomita, H. (2015) Influence of grid aspect ratio on planetary boundary layer turbulence in large-eddy simulations. *Geoscientific Model Development*, 8, 3393–3419.
- Parker, M.D. and Johnson, R.H. (2000) Organizational modes of Midlatitude mesoscale convective systems. *Monthly Weather Review*, 128, 3413–3436.
- Peters, J.M. and Schumacher, R.S. (2016) Dynamics governing a simulated mesoscale convective system with a training convective line. *Journal of the Atmospheric Sciences*, 73, 2643–2664.
- Sato, Y., Nishizawa, S., Yashiro, H., Miyamoto, Y., Kajikawa, Y. and Tomita, H. (2015) Impacts of cloud microphysics on trade wind cumulus: which cloud microphysics processes contribute to the diversity in a large eddy simulation? *Progress in Earth and Planetary Science*, 2, 23. <https://doi.org/10.1186/s40645-015-0053-6>.
- Sekiguchi, M. and Nakajima, T. (2008) A k-distribution-based radiation code and its computational optimization for an atmospheric general circulation model. *Journal of Quantitative Spectroscopy and Radiation Transfer*, 109, 2779–2793.
- Shinoda, T., Amano, T., Uyeda, H., Tsuboki, K. and Minda, H. (2009) Structure of line-shaped convective systems obliquely training to the Baiu front observed around the Southwest Islands of Japan. *Journal of the Meteorological Society of Japan*, 87, 739–745.
- Tomita, H. (2008) New microphysical schemes with five and six categories by diagnostic generation of cloud ice. *Journal of the Meteorological Society of Japan*, 86, 121–142.
- Tsuguti, H. and Kato, T. (2014) Contributing factors of the heavy rainfall event at Amami-Oshima Island, Japan, on 20 October 2010. *Journal of the Meteorological Society of Japan*, 92, 163–183.
- Unuma, T. and Takemi, T. (2016) Characteristics and environmental conditions of quasi-stationary convective clusters during the warm season in Japan. *Quarterly Journal of the Royal Meteorological Society*, 142, 1232–1249.
- Wilson, D.K. (2001) An alternative function for the wind and temperature gradients in unstable surface layers. *Boundary-Layer Meteorology*, 99, 151–158.
- Yoshida, R., Nishizawa, S., Yashiro, H., Adachi, S.A., Sato, Y., Yamaura, T. and Tomita, H. (2017) CONeP: a cost-effective online nesting procedure for regional atmospheric models. *Parallel Computing*, 65, 21–31.
- Yoshizaki, M., Kato, T., Tanaka, Y., Takayabu, H., Shoji, Y. and Seko, H. (2000) Analytical and numerical study of the 26 June 1998 orographic Rainband observed in Western Kyushu, Japan. *Journal of the Meteorological Society of Japan*, 78, 835–856.

## SUPPORTING INFORMATION

Additional supporting information may be found online in the Supporting Information section at the end of the article.

**How to cite this article:** Yoshida R, Nishizawa S, Yashiro H, *et al.* Maintenance condition of back-building squall-line in a numerical simulation of a heavy rainfall event in July 2010 in Western Japan. *Atmos Sci Lett*. 2019;20:e880. <https://doi.org/10.1002/asl.880>